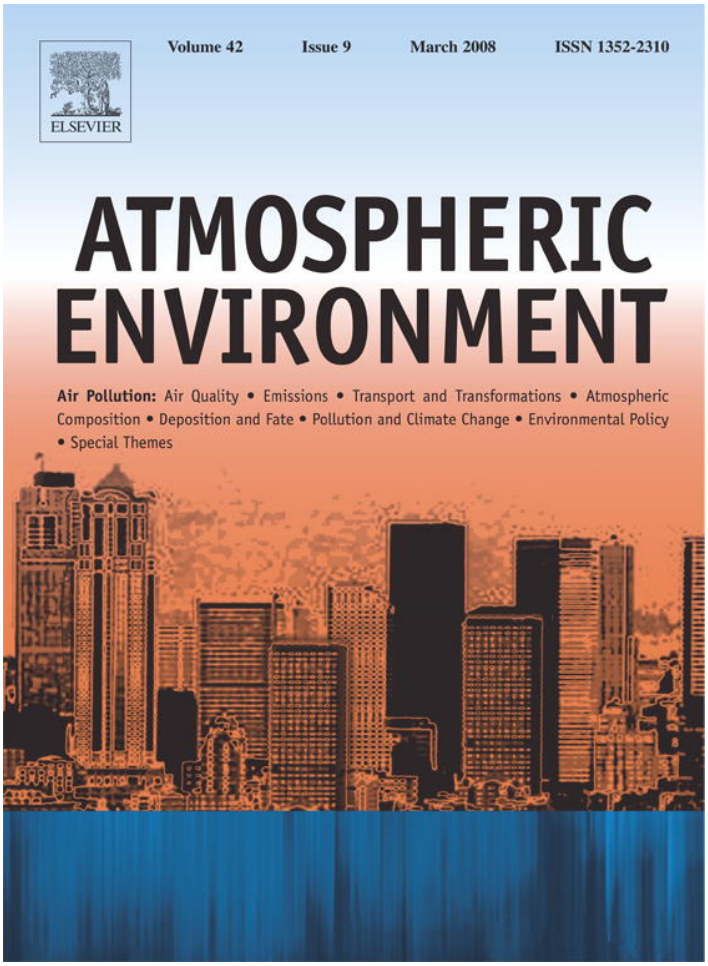

Available online at www.sciencedirect.com
ScienceDirect
Atmospheric Environment 42 (2008) 2007–2022
ATMOSPHERIC ENVIRONMENT
www.elsevier.com/locate/atmosenv

Estimating smoke emissions over the US Southern Great Plains using MODIS fire radiative power and aerosol observations

Nikisa S. Jordan[a,*], Charles Ichoku[b,c], Raymond M. Hoff[a]

[a]*Cooperative Center for Remote Sensing Science and Technology (CREST), Joint Center for Earth Systems Technology (JCET), University of Maryland, Baltimore County 5523, Research Park Drive, Suite 320, Baltimore, MD 21250, USA*
[b]*Earth System Science Interdisciplinary Center (ESSIC), University of Maryland, College Park, MD 20742, USA*
[c]*Climate and Radiation Branch, Code 613.2, NASA Goddard Space Flight Center, Greenbelt, MD 20771, USA*

Received 4 May 2007; received in revised form 16 October 2007; accepted 1 December 2007

Abstract

A newly developed method, which involves the use of satellite measurements of energy released by fires, was used to estimate smoke emissions in the United States (US) Southern Great Plains (SGP). This SGP region was chosen because extensive agricultural and planned burning occurs there annually. Moderate resolution imaging spectroradiometer (MODIS) aerosol optical depth (AOD) and fire radiative energy (FRE) release rates (R_{FRE}), acquired in 2004 from the Terra and Aqua satellites, were used to derive a FRE-based smoke emission coefficient (C_e kg MJ^{-1}), which when multiplied by R_{FRE} (MJ s^{-1}) gives the rate of smoke emission (kg s^{-1}). Correlations between the smoke emission rates and the R_{FRE} were significant for Terra-MODIS ($R^2 = 0.645$, $n = 146$, $p < 0.0001$) and Aqua-MODIS ($R^2 = 0.752$, $n = 178$, $p < 0.0001$). Furthermore, the C_e values derived independently from Terra and Aqua were in close agreement, and the average C_e for this area is 0.049 ± 0.024 kg MJ^{-1}. A Monte Carlo (MC) probabilistic approach was used to approximate uncertainties from the smoke emission and resulting C_e. For the first time, smoke emission estimates have been derived for the US SGP using observations of energy released by fires. Although more work is necessary, the present study demonstrates the feasibility of using R_{FRE} for smoke emission estimation in that region. Burning peaked during the spring and fall seasons. Moreover, qualitative examination of smoke emission patterns side-by-side with local air-quality measurements indicated that the impact of smoke from local biomass burning activities was significant on the regional air-quality.

Keywords: Fire radiative energy (FRE); Smoke; MODIS; Emissions

1. Introduction

Biomass burning is the combustion of organic matter from natural or man-made activities. For anthropogenic uses, it serves as a tool for an array of land-use changes and agricultural management activities (Crutzen and Andreae, 1990; Levine et al., 1995). Humans predominantly initiate burning across the globe, while fires from natural events (lightning induced) occur on a less frequent basis. There are repeating seasonal cycles of biomass burning episodes, but the exact location

*Corresponding author. Tel.: +1 410 455 1942; fax: +1 410 455 1291.
E-mail address: njordan1@umbc.edu (N.S. Jordan).

1352-2310/$ - see front matter © 2008 Elsevier Ltd. All rights reserved.
doi:10.1016/j.atmosenv.2007.12.023

of fires varies each year (Levine, 1991; Levine et al., 1995).

Biomass burning has received attention in the last three decades due to several global and regional concerns about the impact of fire emissions on climate and the environment (Crutzen and Andreae, 1990; Christopher et al., 1998; Kaufman et al., 2003). Although not completely quantified and understood, a strong consensus exists within the scientific community regarding the influence of smoke from biomass burning on climate, health, and air quality (Andreae and Merlet, 2001; Houghton et al., 2001; Kaufman et al., 2002; Lighty et al., 2000). Studies have shown that biomass burning is a major source of atmospheric pollutants (responsible for ~40% of gross carbon dioxide and 38% of tropospheric ozone; Levine et al., 1995). Products such as carbon dioxide, carbon monoxide, methane, nitric oxide, non-methane hydrocarbons, methyl chloride, and primary and oxygenated organic aerosols (POA) are readily emitted from the combustion of vegetation (Levine et al., 1995; Andreae and Merlet, 2001; Kaufman et al., 2002; Keene et al., 2006). These combustion particulates and gases affect the Earth's radiation budget and climate (Levine et al., 1995; Houghton et al., 2001), and several groups have studied the radiative and optical properties of some fire-emitted aerosol species (e.g., Eagan et al., 1974; Penner et al., 1992; Kaufman and Fraser, 1997; Hobbs et al., 1997). Furthermore, aerosols from biomass burning events can affect visibility (Malm, 1999) and do pose a threat to human, animal, and vegetation health (Lighty et al., 2000).

Approximations of fire emission have been frequently derived from estimates of the mass of biomass combusted times an emission factor for the emitted species of interest. Before the satellite era, estimates of smoke emissions were made with the use of models that primarily relied on *in-situ*/field-based inputs (Robinson, 1989). A key study by Wilson and Matthews (1971) offered the first major estimates of total suspended particulate emissions from fire. Similar studies followed (e.g. Wong, 1978; Olson, 1981; Logan et al., 1981), but the work done by Seiler and Crutzen (1980) has been the most cited widely. Robinson (1989) inferred that the study was well received because of detailed documentation and inclusion of necessary parameters. Eq. (1) represents the traditional method for smoke emission estimation (Andreae and Merlet, 2001):

$$M_x = \mathrm{EF}_x M_{\mathrm{biomass}}, \tag{1}$$

where M_x (g) is the mass of the emitted species of interest X, EF_x ($\mathrm{g\,kg^{-1}}$) is the emission factor for X, and M_{biomass} (kg) is the amount of dry fuel consumed.

Emission factors (EF_x) of specific trace substances are generally determined in contained laboratory experiments. However, even if estimates of the emission factor are perfect, one still needs to determine the amount of dry biomass burned (M_{biomass}) before the mass of emitted species (M_x) is known (Andreae and Merlet, 2001). The formula first suggested by Seiler and Crutzen (1980) and still commonly used for estimates of biomass combusted takes the form

$$M_{\mathrm{biomass}} = AB\alpha\beta, \tag{2}$$

where M_{biomass} is the biomass burned (kg), A the total land area burned ($\mathrm{m^2}$), B the biomass loading or fuel density ($\mathrm{kg\,m^{-2}}$), α the fraction of the average above-ground biomass burned, and β the burn efficiency. The high uncertainty in determining each of these parameters makes it difficult to accurately estimate M_{biomass} in the natural environment (Seiler and Crutzen, 1980).

With recent advancement in remote sensing capabilities, interest has been growing on estimating smoke emissions using data from space-borne sensors, which possess the ability to view vast and remote areas. However, implementing fire detection and deriving smoke emissions from satellite observations can be challenging for several reasons. Fires can be missed if they (1) start and end between satellite overpasses, (2) are obstructed by clouds, or (3) are not large or hot enough to be detected by the satellite sensor (Kaufman and Justice, 1998; Kaufman et al., 1998b; Fuller, 2000). Also, many space-borne environmental sensors used to detect fires, such as the Advanced Very High Resolution Radiometer (AVHRR) and the Along Track Scanning Radiometer (ATSR), saturate above 320 °K in the middle infrared and thermal channels, because they were originally designed to measure surface temperatures and cloud radiances, rather than for fire detection. Since most fire events typically range from 400 to 1200 °K (Fuller, 2000), such sensors cannot distinguish between low and high intensity fires. Newer space-borne instruments, such as the moderate resolution imaging spectroradiometer (MODIS) and the bi-spectral infrared detection (BIRD) (an experimental satellite specifically designed to target high temperature events), include specific enhancements for fire detection, which

enables the measurement of fire radiative energy (FRE) release rates (or R_{FRE}), making it possible to distinguish a wide range of fire strengths (Kaufman et al., 1998b, 2003; Justice et al., 1998; Fuller, 2000; Wooster et al., 2003).

The focus of this present study is to estimate the smoke mass flux emitted from biomass burning in the United States (US) Southern Great Plains (SGP) using MODIS R_{FRE} and aerosol optical depth (AOD) measurements. The approach involves implementing the technique developed by Ichoku and Kaufman (2005) to derive the R_{FRE}-based smoke emission coefficients (C_e) for smoke particulate matter (PM), such that measurements of R_{FRE} in the study region at any time can be simply multiplied by the C_e to calculate the rate of PM emission directly. Similarly, if the total FRE released over a given period of time can be estimated from continuous measurements of R_{FRE}, it may be multiplied by C_e to derive total emitted PM for the considered time period (Ichoku and Kaufman, 2005). This technique, also referred to as the "direct approach" for smoke emission estimation, is further described in Section 3. Analysis of the uncertainties associated with this technique has been conducted with careful attention by using the Monte Carlo (MC) approach, which is addressed in Section 4. Lastly, a quantitative assessment of the impact of smoke on air quality within the study region was attempted by examining reconstructed extinction and particle concentrations from the Interagency Monitoring for PROtected Visual Environments (IMPROVE) network.

2. Indirect method of estimating smoke emissions using satellite data

Burned area (parameter A in Eq. (2)) is difficult to determine in the field when using the traditional emission-factor approach for smoke emission estimation (Seiler and Crutzen, 1980). Determination of burned area is also a challenge when using remotely sensed data. It is important to note that burned-area products differ among sensors, resulting in different estimates of smoke emission (Boschetti et al., 2004; Korontzi et al., 2004). Nevertheless, satellite-derived burned-area products and fire pixel counts have been used to indirectly estimate smoke emissions based on Eqs. (1) and (2) (Hely et al., 2003; Simon et al., 2004; Ito and Penner, 2004; Hoelzeman et al., 2004; van der Werf et al., 2006; Soja et al., 2004; Li et al., 2004; Korontzi et al., 2004; Giglio et al., 2006).

Currently, MODIS is showing great potential for providing enhanced burned-area products due to recent improvements in the algorithms (Giglio et al., 2003, 2006). Although that product will likely improve burned-area estimates, improvement in the estimation of the three remaining parameters in Eq. (2) is very difficult (via space borne, *in situ*, or modeling techniques) due to the complexity of the characteristics being quantified (i.e. variability in fuel moisture, loading, and type) (Seiler and Crutzen, 1980; Andreae and Merlet, 2001; Hely et al., 2003; Ichoku and Kaufman, 2005; Roberts et al., 2005; Wooster et al., 2005). Thus, a major issue is that several of those parameters (Eq. (2)) are often estimated with large uncertainties, resulting in inaccurate smoke emission estimation (Wooster et al., 2003, 2005; Korontzi et al., 2004; Roberts et al., 2005; Ichoku and Kaufman, 2005).

Andreae and Merlet (2001) performed a critical analysis of currently available emission data and presented a set of emission factors for a variety of species emitted from burning vegetation. They used extrapolation techniques to estimate values for regions where data were unavailable and concluded that considerable progress has been made for biomass burning emission estimates, although more work is needed (Andreae and Merlet, 2001). The problem is that estimates of the amount of dry fuel consumed ($M_{biomass}$) contain significant errors, which have not been statistically quantified, while EF_x for even fairly well-known species such as CO and CH_4 still have 20–30% uncertainty (Andreae and Merlet, 2001; French et al., 2004). Andreae and Merlet (2001) generalized the uncertainty to be $\pm 50\%$ or greater. Furthermore, correct estimates of regional and inter-annual variations of smoke emissions are necessary before conclusive evaluations can be made of the effects on climate and environment (Scholes and Andreae, 2000; Duncan et al., 2003; Wooster et al., 2003; Ichoku and Kaufman, 2005).

3. A direct method of estimating regional US smoke emissions

Actively burning biomass releases radiative energy, which can be sensed remotely (Kaufman et al., 1998a, b; Wooster, 2002). Fire radiative power (FRP) is its radiative energy rate of release per unit

time (or R_{FRE}), which when integrated over a fire's lifetime yields the total FRE (Wooster et al., 2005).

MODIS is an instrument aboard two NASA satellites, namely Terra and Aqua, launched into orbit on 19 December 1999 and 4 May 2002, respectively. The potential of measuring R_{FRE} using the MODIS instrument was first demonstrated by Kaufman et al. (1998a, b), based on experimental measurements with the MODIS Airborne Simulator (MAS), which flies on a high-altitude aircraft (Kaufman et al., 1998a, b, 2003; Justice et al., 2002). Encouraging results pertaining to the relation of radiative energy to the release of smoke particulates were reported. Also, relationships between R_{FRE} and the spectral properties of fires in the middle and longwave infrared (IR) documented by MAS were exploited to develop an adequate algorithm for the MODIS Earth Observing System (EOS) spaceborne sensor (Giglio et al., 2003).

The energy radiated by a fire is directly proportional to the amount of biomass combusted ($M_{biomass}$) (Roberts et al., 2005; Wooster et al., 2005). Wooster (2002) first showed, in a small-scale field study, the linear relationship ($R^2 = 0.78$) between FRE and $M_{biomass}$. FRE was derived using hyper-spectral observations within the wavelength region of 0.4–2.5 μm (Wooster, 2002). The result of that study was not fully applicable to satellite remote sensing data since derivation of FRE was different from the mid-infrared (MIR)-based approach used for Earth observing missions (Wooster et al., 2003). Recent research by Wooster et al. (2005) was more relevant to EOS sensors like MODIS, because R_{FRE} was derived via hyperspectral and single-waveband (MIR radiance) algorithms using a field-based spectroradiometer and MIR thermal camera. The relationship between the biomass combustion rate ($kg\,s^{-1}$) and R_{FRE} (MW or $MJ\,s^{-1}$) was linear and highly significant ($R^2 = 0.90$). Also, the relationship between biomass combusted (kg) and FRE (MJ) was statistically significant ($R^2 = 0.98$) (Wooster et al., 2005). Thus, FRE and R_{FRE} are proportional to the combustion of vegetation. The linearity of the radiative energy and biomass consumed makes physical sense. For a fixed burn efficiency, a given mass of biomass will release a proportional caloric output upon combustion. FRE and R_{FRE} is a measure of that heat released (albeit the radiant component).

Ichoku and Kaufman (2005) presented a method to determine smoke emissions from biomass burning using MODIS R_{FRE} and AOD measurements. They suggested that given the relationship between the rate of radiative energy release and biomass combusted, Eq. (1) could be rewritten as

$$Q_x = C_e R_{FRE}, \tag{3}$$

where Q_x ($kg\,s^{-1}$) is the satellite-derived smoke emission rate for a given species x, C_e ($kg\,MJ^{-1}$) is its R_{FRE}-based emission coefficient, and R_{FRE} ($MJ\,s^{-1}$) is the rate of release of FRE. The work presented in this paper closely follows the method described by Ichoku and Kaufman (2005) for smoke emission estimation. A synopsis of that approach will be given here. The idea was to test an existing algorithm, in the study area, for R_{FRE} smoke emission estimation to better determine the associated strengths and weaknesses. The method relies on the determination of C_e based on AOD and R_{FRE} data, since AOD can be used to estimate the emitted smoke mass density (SMD). We have, however, been able to pay more attention to quality assurance of the aerosol pixels-containing fire in this assessment, since our study area is smaller and perhaps more homogeneous than most of the regions studied in the prior work. In that study, Ichoku and Kaufman (2005) presented regional analysis results for different parts of the world, which did not include the area of interest in this study: the US SGP. The area is bounded by the coordinates 32.0°N, 40.0°N, 102.0°W, 90.0°W (delineated with the black box in Fig. 1) and was chosen due to the frequent occurrence of annual biomass burning (Reid et al., 2004). The fuel type of this region primarily consists of grasslands, croplands, and deciduous broadleaf trees (Fig. 1), fire events are mostly due to prescribed and agricultural burning activities (planned burning), which particularly occur in the spring season (late February–May). These events are significant contributors to smoke dominated haze (Reid et al., 2004) in the region and can also be transported downwind of the events.

3.1. Satellite data analysis

In this study, data from the MODIS instrument aboard the Aqua and Terra satellites were acquired and analyzed for 2004. Both Terra-MODIS and Aqua-MODIS achieve almost a full global coverage once in the daytime and once at night. Only the daytime data will be used in this study, since MODIS measures AOD only during the day. It is important to note that observations made by these

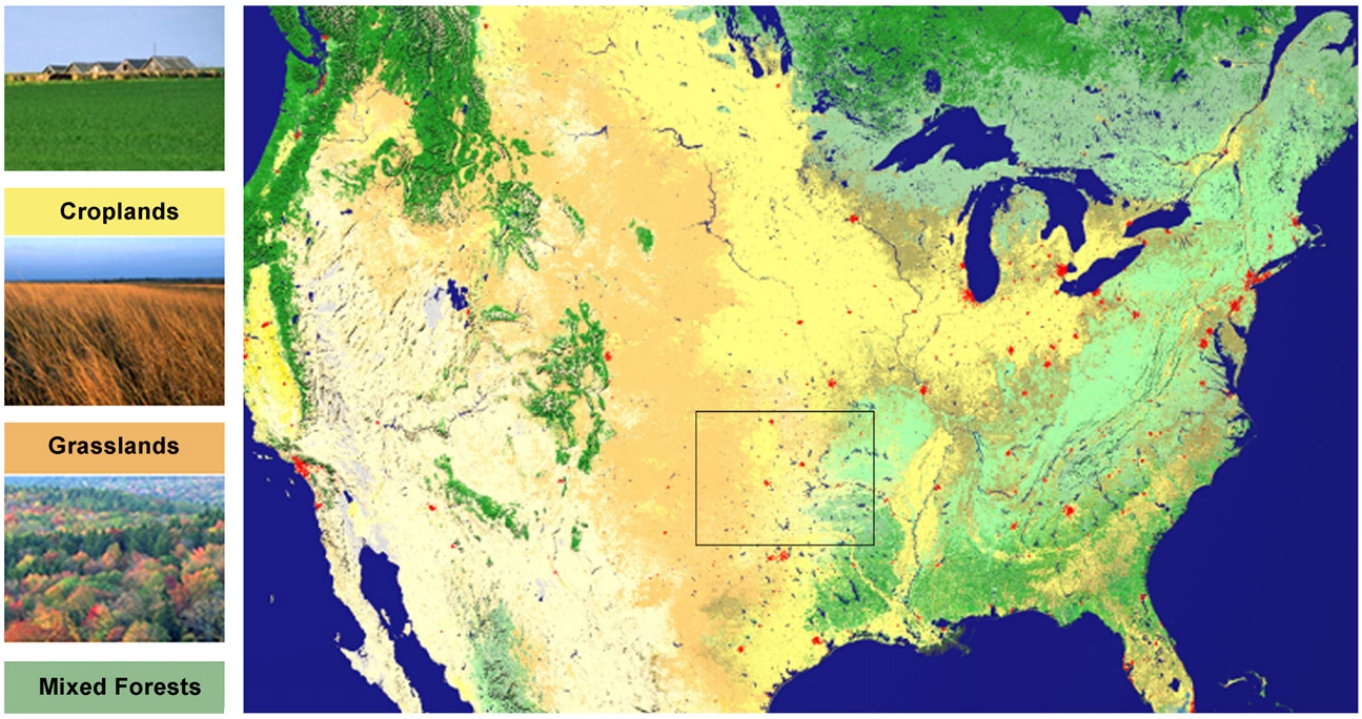

Fig. 1. Land cover map of the contiguous US regions generated by Boston University and NASA Goddard Space Flight Center, which is based on MODIS (November 2000–October 2001) data. The map was sourced from the NASA Earth Observatory (NASA News Archive, Release NO: 02-126, 13 August 2002, http://earthobservatory.nasa.gov/Newsroom/LCC/) and edited to show the region studied in this research.

polar orbiting satellites are near instantaneous. More specifically, Terra-MODIS views the SGP in the mid morning (~11:00 am CST) and Aqua-MODIS views the surface in the early afternoon (~1:00 pm CST). The MODIS Level 2 fire product (MOD14-Terra and MYD14-Aqua) was used to identify fire occurrence, location, and intensity. Fires are observed by MODIS at a spatial resolution of 1 km at nadir (Kaufman and Justice, 1998; Kaufman et al., 2003). The MODIS AOD product (MOD04-Terra and MYD04-Aqua), provided at 10-km resolution at nadir (Kaufman and Tanre, 1998), was used to determine smoke aerosol column loadings. AOD is a measure of light attenuation by aerosols along a vertical column. Values typically range from 0.0 to 5.0. Measurements greater than one indicate significant haze and greater than two indicate extremely intense haze or smoke events (Chu et al., 2003). All instances of fire (at $1 \times 1\,km^2$ resolution) within each aerosol pixel (at $10 \times 10\,km^2$ resolution) were counted and the rate of FRE (R_{FRE}) related to each fire pixel was also totaled. Therefore, every aerosol pixel containing fire(s) has an associated subtotaled measure of R_{FRE} and fire occurrence. The next step was to use the AOD in conjunction with the wind speed near the source to determine a flux of smoke from the source. The wind field data used were obtained from the National Center for Environmental Prediction/National Center for Atmospheric Research (NCEP/NCAR) reanalysis system (Kalnay et al., 1996; Kistler et al., 2001).

Estimating smoke emission from fires via the Ichoku and Kaufman (2005) method continues by determining the column SMD. To do this, the AOD of aerosol pixels surrounding the central aerosol pixel that contains fire were determined. The aerosol pixel that contains the smallest AOD value was considered the relative background ($\tau_a^{background}$) and the aerosol pixel with the highest AOD value was considered to contain the total smoke emitted from the fire plus the relative background (τ_a^{total}). Thus, the AOD of smoke emitted as a result of fire(s) within an aerosol pixel is

$$\tau_a^{smoke} = \tau_a^{total} - \tau_a^{background}, \quad (4)$$

where τ_a^{smoke} is the optical depth of emitted smoke, τ_a^{total} is the maximum loading of smoke, which includes the relative background, and $\tau_a^{background}$ is the optical thickness of the background.

For estimation of column SMD, it is important to determine an appropriate smoke mass extinction

efficiency α_e ($m^2\,g^{-1}$) for the biomass type in the area of interest. Smoke mass extinction efficiency, α_e ($m^2\,g^{-1}$), is the sum of the smoke mass scattering (α_s) and absorption (α_a) efficiencies (Reid et al., 2005a, b). A critical study by Reid et al. (2005b) presented a detailed review of the optical properties of biomass burning particles. In that study, Reid et al. (2005b) reported the likely optical properties for dry burning of grasslands/savannas at the 550 nm wavelength. For "fresh smoke" (~5 min old) the efficiencies were $\alpha_s \sim 3.6 \pm 0.4\,m^2\,g^{-1}$ and $\alpha_a \sim 0.8 \pm 0.3\,m^2\,g^{-1}$. Optical measurements for "aged smoke" (ranges from 1 h to several days) were $\alpha_s \sim 4.0 \pm 0.4\,m^2\,g^{-1}$ and $\alpha_a \sim 0.65 \pm 0.3\,m^2\,g^{-1}$. Consequently, the smoke mass extinction efficiency for fresh smoke would be $4.4 \pm 0.5\,m^2\,g^{-1}$ and for aged smoke $4.65 \pm 0.5\,m^2\,g^{-1}$. In this study, we adopted the value of $\alpha_e = 4.5 \pm 0.5\,m^2\,g^{-1}$ because it is the median measure for fresh and aged smoke for fuel types similar to the US SGP. Furthermore, a recent study by Wang and Christopher (2006) used $\alpha_e = 4.5\,m^2\,g^{-1}$ for this area. Thus, SMD on a pixel-by-pixel basis was calculated as follows (Ichoku and Kaufman, 2005):

$$\mathrm{SMD} = \tau_a^{\mathrm{smoke}}/\alpha_e, \tag{5}$$

where SMD is in $g\,m^{-2}$, τ_a^{smoke} (unitless) is the optical depth of emitted smoke shown in Eq. (4) and α_e ($m^2\,g^{-1}$) is the smoke mass extinction efficiency.

In order to determine the flux of smoke out of each aerosol pixel-containing fire for which the SMD was determined, wind fields from the NCEP/NCAR reanalysis data set were used to determine the clearance time, t_{clear} (or the time for a pixel to be cleared of smoke), $L/|\mathbf{u}|$, where L is the length of the pixel (i.e. the travel path of the wind across the pixel) and $|\mathbf{u}|$ is the mean wind speed at plume altitude. A simple box model will show that the smoke PM (or aerosol) column mass density times the pixel area divided by the clearance time will be the mass emission rate, Q_{PM} ($kg\,s^{-1}$) (see Eq. (9)), which is equivalent to R_{SA} in Ichoku and Kaufman (2005).

3.2. Quality control (QC)

At this point of analysis, four parameters for every aerosol pixel-containing fire have been determined. The next step was to incorporate QC to strengthen the analysis.

The MODIS fire product includes a detection confidence estimate for every 1 km^2 fire pixel. It was developed to help users assess the confidence of detected fires. However, the latest version of MODIS fire product available at the time of this work (Collection 4) does not effectively recognize highly questionable fires. Therefore, the fire confidence parameter was not utilized for QC measures in this study. Issues with this parameter will be rectified in the MODIS Collection 5 fire product (Giglio, 2005). Careful analysis of some MODIS true color images of fire scenes in the area showed that there were fire pixels for which no smoke was evident even at the $1 \times 1\,km^2$ scale. This was particularly noted at the edges of the MODIS swath. While it is beyond the scope of this work to analyze why the fire detection algorithm identified these pixels as fire, it is noteworthy that glint over small lakes, hot surfaces, and other types of noise could all give false positives in the fire detection (Giglio, 2005).

The primary QC strategy applied here was to remove all fire pixels that did not have an associated SMD. This means that there was an aerosol pixel that contained fire(s) but the column SMD could not be derived since AOD was not retrieved (missing data). It is believed that derivation of C_e based only on coincidences of smoke emission and FRE will help reduce errors due to fire-detection false alarms. The results derived before and after QC measures are reported in Section 5.

3.3. Deriving the smoke aerosol emission coefficient C_e

To derive C_e for our study area, all aerosol pixels-containing fires were clustered on a daily basis. It is important to note that all the satellite observations were acquired almost instantaneously during each overpass. For each overpass time, the total number of aerosol pixels that had fire(s) with aerosol retrieval is denoted by N_{aero}, and the total R_{FRE} (MW or $MJ\,s^{-1}$) is given by

$$R_{\mathrm{FRE}} = \sum_{i=1}^{N_{\mathrm{aero}}} R_{\mathrm{FRE}_i}, \tag{6}$$

where the subscript i is a counter that designates the R_{FRE} values for individual fire-containing aerosol pixels. The total area (A_T km^2) of fire influence within the region of interest was derived by summing the areas of these pixels:

$$A_T = \sum_{i=1}^{N_{\mathrm{aero}}} P_{\mathrm{area}_i}. \tag{7}$$

The total column SMD (described in Section 3.1) associated with all aerosol pixels-containing fire was calculated on a daily basis. Dividing it by N_{aero} yields $\langle SMD_T \rangle$ (kg km^{-2}), which is the average of column SMD at the time of overpass for the region of interest:

$$\langle SMD_T \rangle = \frac{(\sum_{i=1}^{N_{aero}} SMD_i)}{N_{aero}}. \quad (8)$$

Multiplying the average SMD ($\langle SMD_T \rangle$) by total area (A_T) of observed fire and dividing by the average time of emission (t_{clear}) yields the average smoke PM emission rate (Q_{PM} in kg s^{-1}):

$$Q_{PM} = \frac{\langle SMD_T \rangle \times A_T}{\langle t_{clear} \rangle}. \quad (9)$$

The final step in determining C_e was to generate a scatter plot of Q_{PM} against R_{FRE} and perform a zero-intercept linear regression fit (Ichoku and Kaufman, 2005).

4. Error analysis

It is obvious from this study and many others that the accuracy achieved in evaluating the impact of smoke on air quality, health, and climate is dependent on the accuracy of estimation of smoke emissions. Since there are primarily two (direct and indirect) methods used to estimate smoke emissions from spaceborne fire observations, a comparison of the percentage error associated with each method will provide a quantitative measure of the relative uncertainties. The focus of this section is to analyze the errors associated with each smoke emission technique (direct and indirect) in an effort to evaluate their reliability. The most challenging part of the error analysis is the ability to achieve accurate determination of errors associated with each parameter before performing the error propagation. In the present analysis, appropriate logical assumptions and previously published errors will be used.

4.1. Indirect method

According to Andreae and Merlet (2001), the uncertainties associated with the EF_x for many significant species (i.e. CO and CH_4) have improved since the Seiler and Crutzen (1980) study, and they estimated them to be presently around 20–30%. At the time of their study, Andreae and Merlet (2001) noted that there was not enough information available to determine a statistically valid error related to $M_{biomass}$. Therefore, a general assumption of $\pm 50\%$ uncertainty was made (Andreae and Merlet, 2001).

Recent studies (e.g., Korontzi et al., 2004; Li et al., 2004) have used MODIS-derived burned area (parameter "A" in Eq. (2)) in conjunction with other inputs (i.e. fuel load and combustion completeness) to estimate $M_{biomass}$. Unfortunately, none of these studies critically documented the average error associated with MODIS-derived burned area (i.e. $\pm$percentage uncertainty was not given). The MODIS-derived burned area (via the bidirectional reflectance model-based change detection algorithm) product will not become available to the community until late 2007. Thus, research is currently underway to investigate caveats and known problems (Roy et al., 2006).

4.2. Direct method

A Monte Carlo (MC) probabilistic approach (Penman et al., 2000) was used to approximate calculated smoke mass flux uncertainties related to this study. Furthermore, the uncertainty related to the calculated smoke mass flux (Eq. (9)) was determined using different combinations of randomly sampled values from the input parameters. More specifically, the idea was to sample randomly from the known and measured probability distributions of the input variables and to feed combinations of the sampled values into the function (Eq. (9)). This process was repeated 10,000 times.

A program based on the Statistical Analysis Software (SAS) system was created to implement the uncertainty model. SAS is a statistical software package developed for analytic research (Fan et al., 2002). Almost all of the input parameters, which include, τ_a^{smoke}, L, u, and t_{clear} had lognormal distributions. After reviewing the MODIS geolocation error analysis results presented by Wolfe et al. (2002), random errors associated with A_T were assumed to be at least 10%. The smoke extinction efficiency ($\alpha_e \sim 4.5 \pm 0.5$ m^2 g^{-1}) used from published literature (Reid et al., 2005b; Wang and Christopher, 2006) was assumed to follow a normal distribution.

5. Results

5.1. Smoke mass flux and R_{FRE}-based smoke emission coefficients (C_e)

Measurements of R_{FRE} and AOD from both Aqua- and Terra-MODIS were used to determine smoke emitted in the US SGP. Emission estimates were derived for the entire year of 2004. Fig. 2a (Terra) and 2b (Aqua) illustrate the regional R_{FRE}-based smoke PM emission coefficient (C_e). These plots represent the data set after QC measures and correspond to wind speeds at 850 mb (~1.5 km) atmospheric pressure. The vertical error bars shown in Fig. 2a and b correspond to the standard error of smoke emission (standard deviation/$\sqrt{n}$).

Before QC, the Terra data set contained 196 daily observations ($n = 196$) of fire and smoke. After QC this number was reduced to 146 ($n = 146$). Thus, the reduction due to QC is 25%. Aqua MODIS had more daily observations of fire and smoke. More specifically, $n = 230$ before QC and decreased to $n = 178$ after QC. For this data set, the reduction in daily averaged sample size due to QC is 22%.

Correlations between Q_{PM} and R_{FRE} were significant ($0.46 < R^2 < 0.75$, $p < 0.0001$) at the three

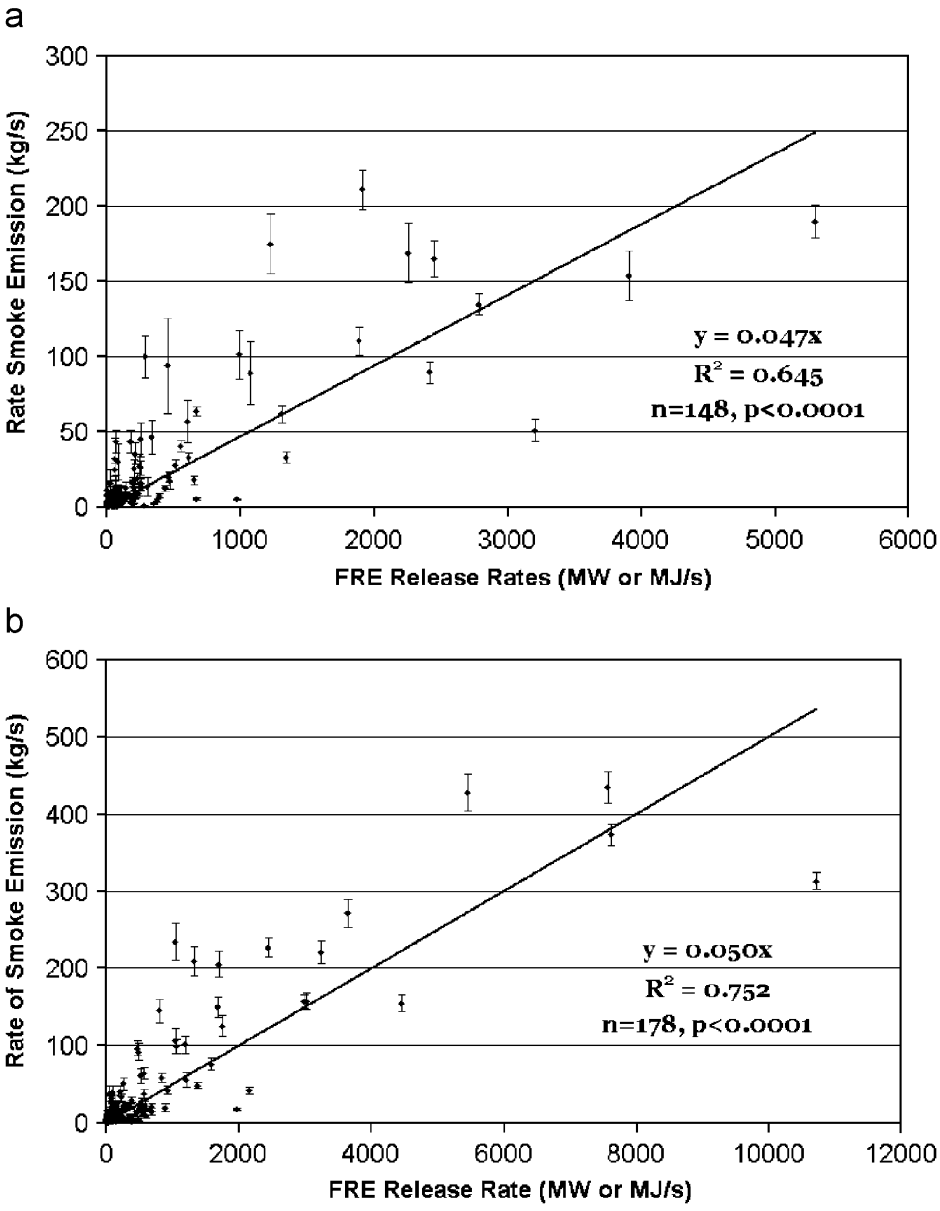

Fig. 2. (a) Terra and (b) Aqua MODIS after quality control measures. Shown is the regional comparison of daily FRE release rates (MW or MJ s^{-1}) and smoke emission (kg s^{-1}) at 850 mb (1.5 km). The slope of the regression line represents the FRE-based smoke emission coefficient (C_e). Vertical error bars represent the standard error of smoke emission.

wind levels considered (700, 850, and 925 mb, equivalent to ~3, ~1.5, and 0.75 km heights, respectively). Variability in both data sets (Terra and Aqua) decreased after the QC measures (Table 1). The slope of the linear regression fit represents the C_e as determined from each data set. It was evident that the C_e's were similar with wind speeds at 850 and 925 mb pressure levels (Table 1). Fires observed in this area are not likely to inject smoke high into the atmosphere (we expect these plumes to be within the Planetary Boundary Layer (PBL)), because their sizes are limited by the burning practice. Therefore, the C_e's derived with wind speeds at 850 mb are assumed to be suitable for estimating smoke emission in the study region. It is noteworthy that although the C_e values were calculated independently from Terra and Aqua, they show a very strong agreement. The overall average C_e (at 850 mb) for the US SGP region studied, based on the 2004 Terra- and Aqua-MODIS Collection 4 data used in this work, is $0.049 \pm 0.024\,\mathrm{kg\,MJ^{-1}}$.

Ichoku and Kaufman (2005) first described the method employed in this study for smoke emission estimation in different regions of the world, and noted that the R_{FRE}-based coefficient of smoke emission (C_e) differed from region to region. The primary cause for this variation was due to the dominant ecosystem (i.e. land cover types) associated with each region. As explained earlier, the major vegetation types of the region analyzed (US SGP) consist of grasslands, croplands, and deciduous broadleaf trees. Ichoku and Kaufman reported a range of C_e ($0.048 < C_e < 0.076$) values for savanna and grassland regions. The average C_e ($0.049 \pm 0.024\,\mathrm{kg\,MJ^{-1}}$) derived in this study was within that estimate made by Ichoku and Kaufman (2005).

Table 1
Calculated Terra and Aqua MODIS R_{FRE}-based coefficients of smoke emission (C_e) and corresponding R^2 for wind speeds taken at different pressure levels (alts)

	C_e	R^2
Terra MODIS		
After quality control		
925 mb (~0.75 km)	0.045	0.457
850 mb (~1.5 km)	0.047	0.645
700 mb (~3 km)	0.062	0.709
Before quality control		
925 mb (~0.75 km)	0.052	0.474
850 mb (~1.5 km)	0.051	0.549
700 mb (~3 km)	0.063	0.669
Aqua MODIS		
After quality control		
925 mb (~0.75 km)	0.044	0.749
850 mb (~1.5 km)	0.050	0.752
700 mb (~3 km)	0.086	0.726
Before quality control		
925 mb (~0.75 km)	0.045	0.703
850 mb (~1.5 km)	0.051	0.705
700 mb (~3 km)	0.083	0.681

Time series plots of Q_{PM} (Eq. (9)) and R_{FRE} (Eq. (6)) for both data sets (Terra and Aqua) show a prominent seasonal pattern, with burning peaking during the spring and fall seasons (Fig. 3), which coincided with other fire analysis studies for this region (Reid et al., 2004). Agricultural and planned burning activities are the major drivers of this pattern. More precisely, prescribed burning is conducted during the spring and fall seasons due to favorable biological and climatological conditions, while agricultural burning occurs before seeds are sown in the spring and after the fall harvest (Reid et al., 2004).

In general, Aqua-MODIS observed more fires and smoke than Terra-MODIS (Fig. 3), implying that there is more burning activity in the afternoon than in the morning. Terra first views the US SGP in the morning (~17:00 UTC or ~11:00 am CST), while Aqua follows with an afternoon overpass (~19:00 UTC or ~1:00 pm CST). Fig. 4 displays all 2004 aerosol pixels-containing fire(s) for both Terra- and Aqua-MODIS, showing that fires are more frequent in the eastern half of Kansas and Oklahoma. Extensive burning is also evident in Arkansas. Fires, due to burning of private rangelands, occur more frequently in Oklahoma and Kansas. Prescribed burning of publicly managed grasslands and forest were likely the primary causes for fire activity in Arkansas (Reid et al., 2004).

5.2. Uncertainty model

Uncertainties associated with the calculated smoke emission estimates (Eq. (9)) were, on average, 47%. Error linked to the estimation of t_{clear} (time for a pixel to be cleared of smoke) and column SMD is the most significant. The coefficient of variation (standard deviation/mean × 100) was, on average, 30% for each of these parameters. Thus, t_{clear} and SMD errors dominated the uncertainty related to the calculated smoke mass flux.

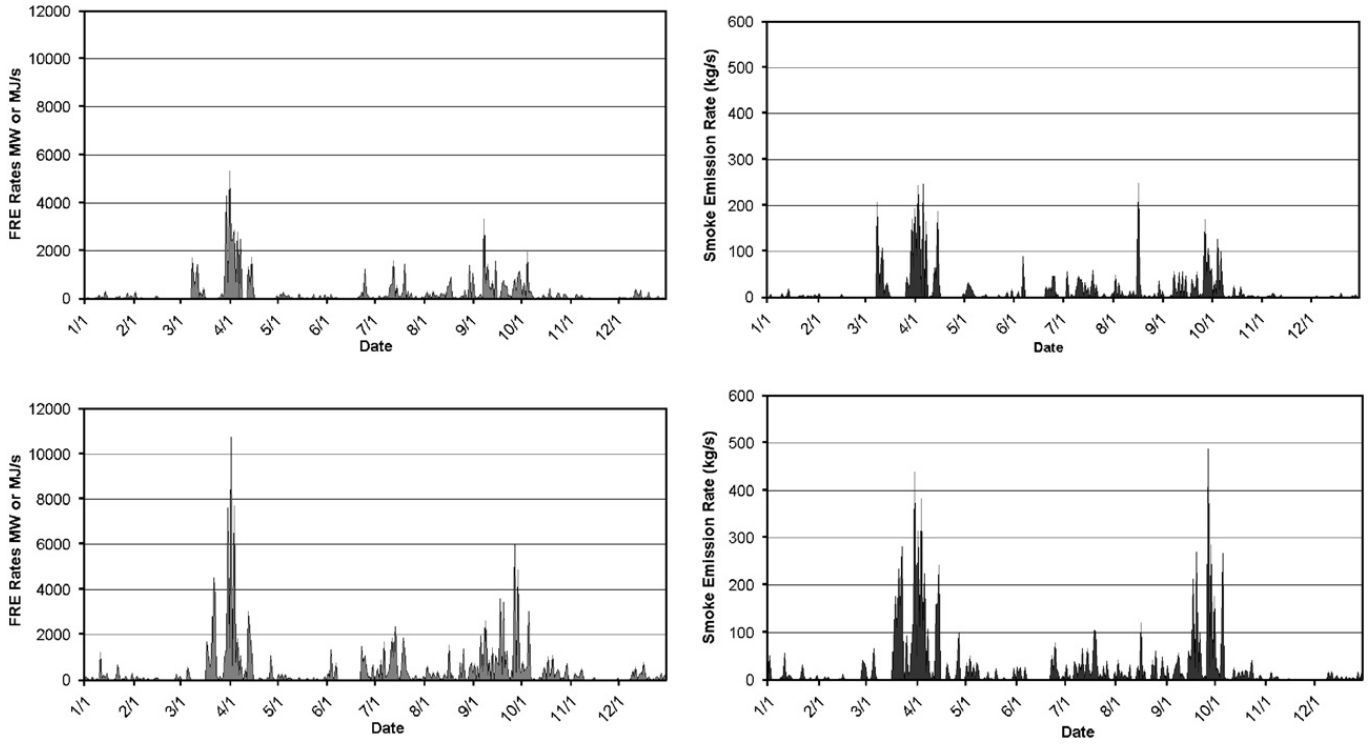

Fig. 3. Comparison of 2004 regional fire and smoke emission from Terra (top panel) and Aqua MODIS (bottom panel). The time series graphs on the left display the instantaneous daily FRE release rates (MW or $MJ\,s^{-1}$) and the plots on the right show the daily instantaneous average smoke emission rates Q_{PM} ($kg\,s^{-1}$). In most cases, Aqua observed twice as much fire and smoke emission as Terra.

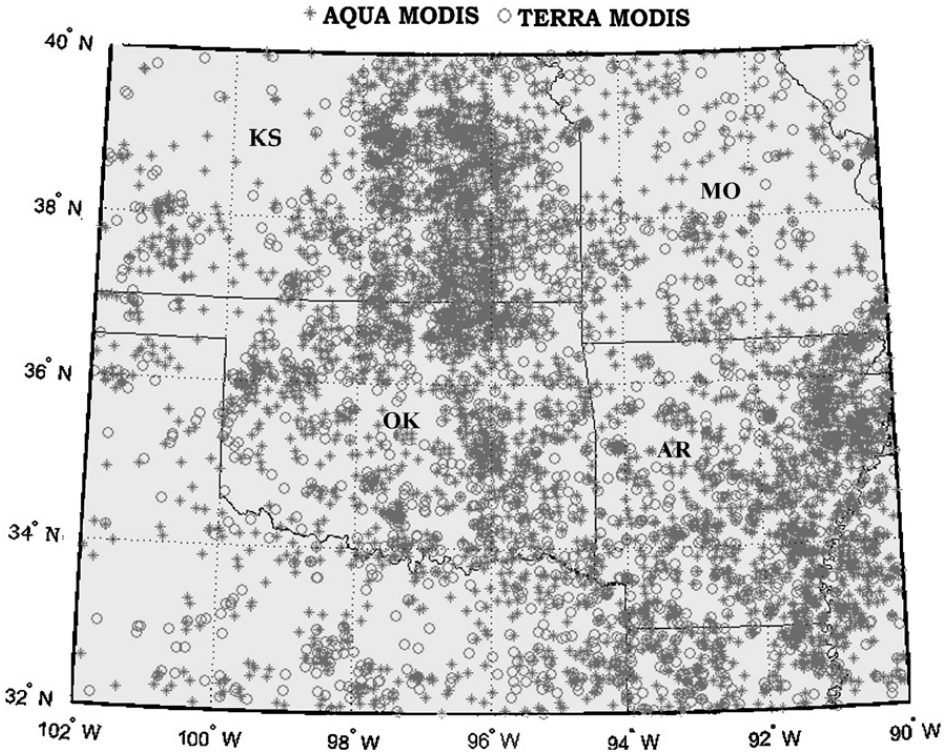

Fig. 4. All aerosol pixels-containing fire(s) observed by Terra and Aqua MODIS for 2004.

Propagating errors connected to Q_{PM} (47%) and R_{FRE} yielded the C_e uncertainty. Ambiguity associated with MODIS R_{FRE} observations has not been critically quantified for the US SGP. However, simulations have been used to show the sensitivity of the MODIS fire algorithms to R_{FRE} (Kaufman and Justice, 1998). According to the MODIS fire algorithm technical background document (ATBD) the relative percent error in R_{FRE} ranges from 7% to 38%, of which the larger uncertainties were related to smaller fires (Kaufman and Justice, 1998). Thus, the average error of MODIS R_{FRE} is 16%, which therefore indicates that the average R_{FRE}-based smoke C_e is 0.049 ± 0.024 or 49%. Therefore, error related to predicting Q_{PM} (Eq. (3)) from the model, using the derived C_e, ranges from 49% to 62%. This range of uncertainty is directly related to fire size.

Table 2
Coordinates of protected IMPROVE sites within the study region

Site name	Site code	State	Latitude (DD)	Longitude (DD)
Tallgrass	TALL1	KS	38.43	−96.56
Hercules Glades	HEGL1	MO	36.61	−92.92
Upper Buffalo Wilderness	UPBU1	AR	35.82	−93.20

6. Qualitative assessment of the impact of smoke on local air quality

Measurements from the IMPROVE program were analyzed to investigate agreement between ground-based particulate observations and the satellite-derived smoke emission estimates presented in this study. More precisely, IMPROVE reconstructed fine particulate mass and extinction values are reported to provide an enhanced understanding of surface air quality. The IMPROVE reconstructed extinction equation used to estimate light scattering and absorption as a result of particles in the atmosphere is further explained by Malm et al. (1994, 2004) and Malm and Hand (2007). Similarly, a description of the protocols used to determine reconstructed fine particulate mass (aerodynamic diameter $<2.5\,\mu m$ or $PM_{2.5}$) concentrations is provided (Malm et al., 1994, 2004; Malm and Hand, 2007). The IMPROVE data used in this study are available online at http://vista.cira.colostate.edu/views/Web/General/DataResources.htm and were obtained on 3 April 2007.

Three IMPROVE protected sites were chosen within the area studied for smoke emission estimation, namely, Upper Buffalo Wilderness (UPBU1), Hercules-Glades (HEGL1), and Tallgrass (TALL1), as shown in Table 2 and Fig. 5. A time series plot of

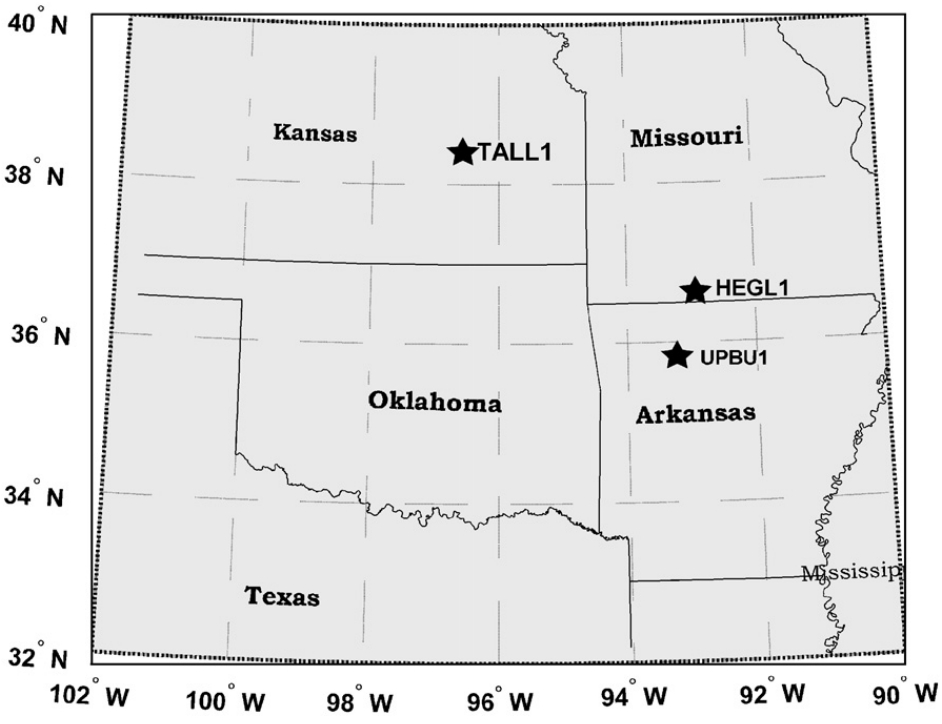

Fig. 5. Region analyzed for smoke emission estimation. Local Interagency Monitoring for PROtected Visual Environments (IMPROVE) sites are also displayed.

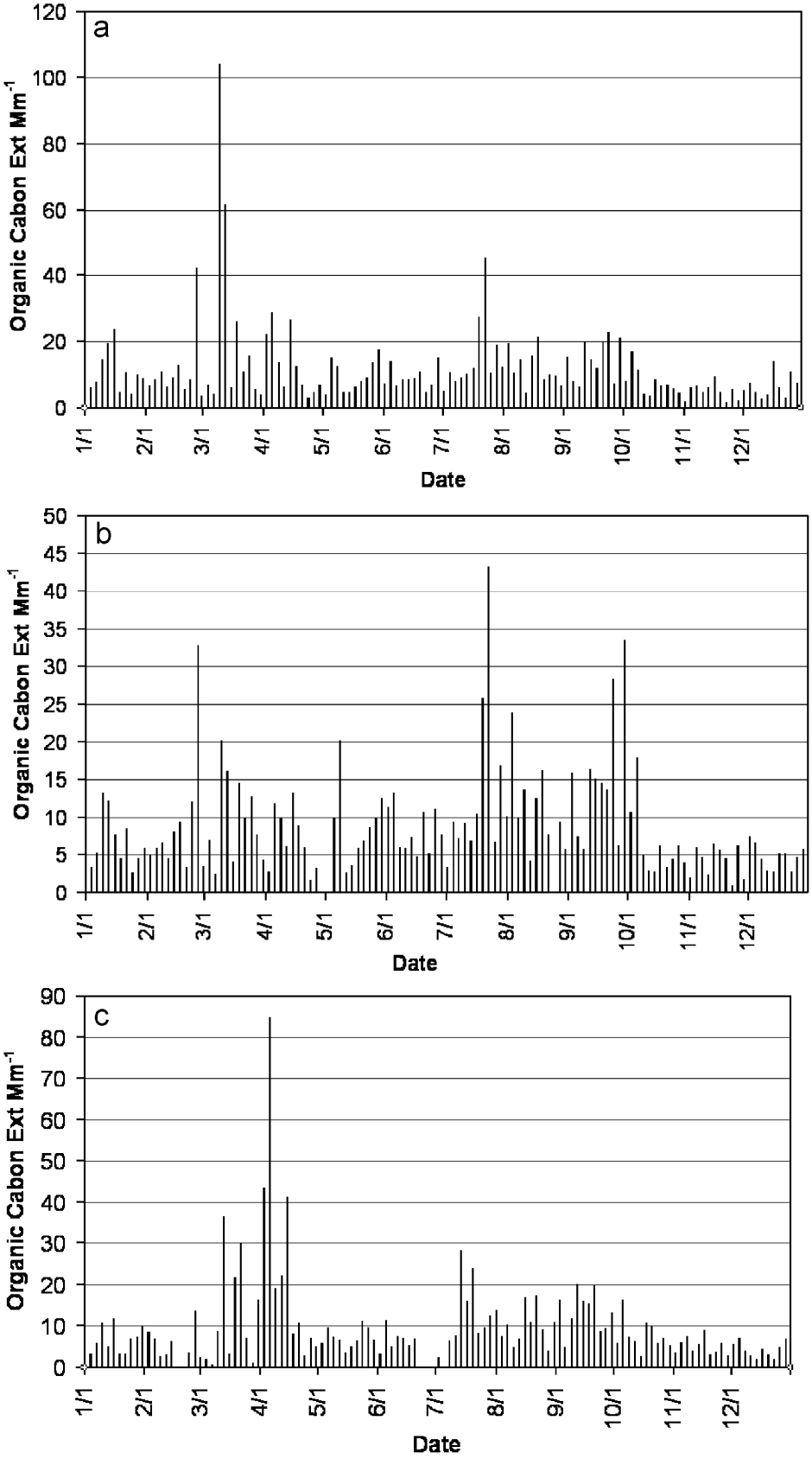

Fig. 6. Protected IMPROVE sites within the study region: (a) Hercules-Glades, (b) Upper Buffalo Wilderness, and (c) Tallgrass with daily measurements of organic carbon extinction for 2004.

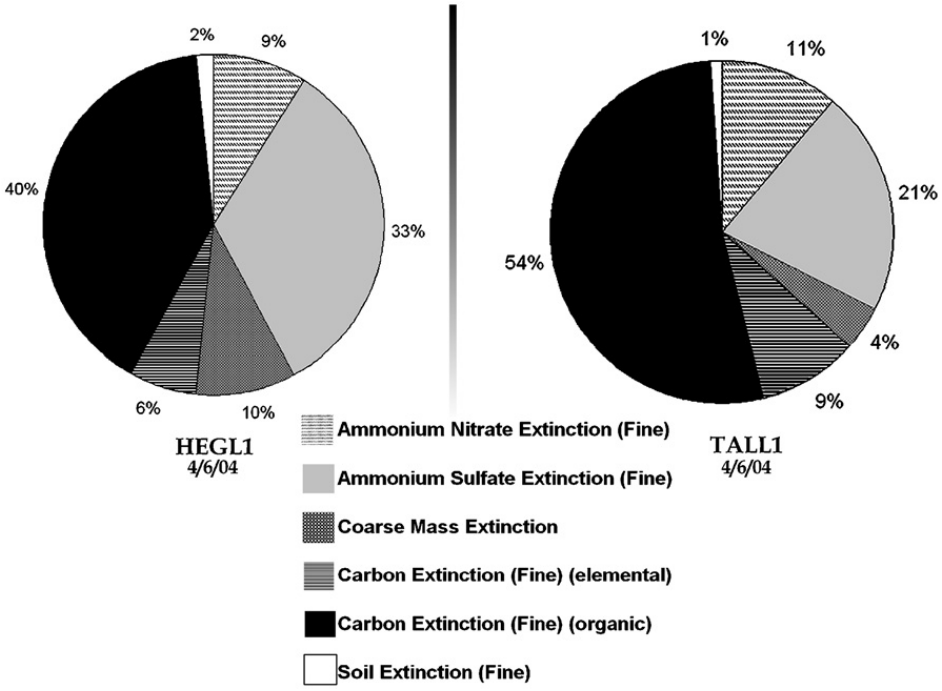

Fig. 7. Extinction fraction for Hercules-Glades and Tallgrass for 6 April 2004.

daily measurements of organic carbon (OC) extinction from the three sites was generated (Fig. 6). The time series graph showed a similar seasonal pattern to that of smoke emission rates as derived in this study (Fig. 3). This suggests a significant impact of the regional biomass burning smoke on the local air quality. The coincidence of smoke-related particulates was most significant on 6 April 2004 at HEGL1 and TALL1. The estimated R_{FRE}-related smoke mass flux at 850 mb for 6 April 2004 is 205 $kg\,s^{-1}$. Furthermore, the IMPROVE OC extinction was 28.8 Mm^{-1} at HEGL1 and 84.7 Mm^{-1} at TALL1, while their corresponding OC fine PM were 7.21 and 21.1 $\mu g\,m^{-3}$, respectively (Malm et al., 1994, 2004). Fig. 7 consists of pie diagrams for 6 April 2004 showing the percentages of IMPROVE reconstructed light extinction for various aerosol components at HEGL1 and TALL1, which include OC, ammonium sulfate, soil, ammonium nitrate, and elemental carbon (Malm et al., 1994). The predominance of organic mass in the extinction apportionment is rare and clearly indicates a smoke source. Thus, the extinction values were indicative of a smoky day in the region studied and correspond to the observed peak of smoke emission via the MODIS satellite technique used. A similar coincidence was also evident during the fall burning period.

7. Conclusion

For the first time, smoke emission estimates by way of MODIS FRE release rates (R_{FRE}) have been presented for the US SGP. The methodology follows the approach presented by Ichoku and Kaufman (2005) for smoke emission estimation. Results in this research showed that burning peaked during the spring and fall seasons, which agreed with other fire studies specific to this region (Reid et al., 2004). The average C_e derived ($0.049 \pm 0.024\,kg\,MJ^{-1}$) was comparable to results published by Ichoku and Kaufman (2005) for similar fuel types. Results also indicated that fires were most frequent in Kansas and Arkansas.

Several lessons were learned after the regional fire analysis. First, it is better to study small areas with minimum variability in fuel types rather than large regions based on geographical convenience. In their global study, Ichoku and Kaufman (2005) noted that a R_{FRE}-based smoke emission coefficient could not be adequately derived for the entire US. This is to be expected since fuel type and terrain (Fig. 1) vary significantly across the US. Also, the accuracy of MODIS AOD (Collection 4) used in this study varies across the country; being particularly poor over bright surfaces. Similarly, the accuracy of fire detection and measurement by MODIS differs from

region to region (Giglio et al., 2003, 2006; Giglio, 2005).

Estimating smoke emissions via the direct approach is promising although more work is needed to minimize error. A MC probabilistic approach was used to propagate uncertainties. Moreover, error related to predicting Q_{PM} (Eq. (3)) from the model, using the derived C_e, ranges from 49% to 62%, which is similar to the smoke emission uncertainty ($\pm 50\%$) postulated by Andreae and Merlet (2001) for the indirect technique. We found that error related to the estimation of t_{clear} (time for a pixel to be cleared of smoke) and column SMD to be the most significant. Minimizing errors in transport wind speed and improving the AOD retrieval will be most effective in improving the reliability of the smoke mass flux approximations.

Lastly, for future studies, we also plan to extend the presented method throughout the US (and perhaps into other parts of North America), in order to estimate C_e values, which will be beneficial for air quality applications at least across the contiguous US. Furthermore, since geostationary satellites have a much higher temporal frequency than polar orbiters such as MODIS, it may be beneficial to integrate MODIS R_{FRE} measurements with Geostationary Operational Environmental Satellites (GOES) observations, for the area studied. This will likely enable estimation of total emissions for any given period of time (as distinct from instantaneous emission rates) and forms part of the future plans for this work.

Acknowledgments

This study was supported and monitored by National Oceanic and Atmospheric Administration (NOAA) under Grant NA06OAR4810162. The views, opinions, and findings contained in this paper are those of the authors and should not be construed as an official National Oceanic and Atmospheric Administration or US Government position, policy, or decision.

References

Andreae, M.O., Merlet, P., 2001. Emission of trace gases and aerosols from biomass burning. Global Biogeochemical Cycles 15, 955–966, 2000GB001382.

Boschetti, L., Eva, H.D., Brivio, P.A., Gregoire, J.M., 2004. Lessons to be learned from the comparison of three satellite-derived biomass burning products. Geophysical Research Letters 31, L21501.

Christopher, S.A., Wang, M., Berendes, T.A., Welch, R.M., Yang, S.K., 1998. The 1985 biomass burning season in South America: satellite remote sensing of fires, smoke, and regional radiative energy budgets. Journal of Applied Meteorology 37 (7), 661–678.

Chu, D.A., Kaufman, Y.J., Zibordi, G., Chern, J.D., Mao, Jietai, Li, Chengcai, Holben, B.N., 2003. Global monitoring of air pollution over land from the Earth Observing System—Terra Moderate Resolution Imaging Spectroradiometer (MODIS). Journal of Geophysical Research 108 (D21), 4661.

Crutzen, P.J., Andreae, M.O., 1990. Biomass burning in the tropics: impact on atmospheric chemical and biochemical cycles. Science 250, 1669–1678.

Duncan, B.N., Martin, R.V., Staudt, A.C., Yevich, R., Logan, J.A., 2003. Interannual and seasonal variability of biomass burning emissions constrained by satellite observations. Journal of Geophysical Research 108 (D2), 4100.

Eagan, R.C., Hobbs, P.V., Radke, L.F., 1974. Measurements of cloud condensation nuclei and cloud droplet size distributions in the vicinity of forest fires. Journal of Applied Meteorology 13, 553–557.

Fan, X., Felsovalyi, A., Sivo, S.A., Keenan, S., 2002. SAS for Monte Carlo Studies: A Guide for Quantitative Researchers. SAS Institute, Cary, NC.

French, N., Goovaerts, P., Kasischke, E.S., 2004. Uncertainty in estimating carbon emissions from boreal forest fires. Journal of Geophysical Research 109.

Fuller, D.O., 2000. Satellite remote sensing of biomass burning with optical and thermal sensors. Progress in Physical Geography 24, 543–561.

Giglio, L., 2005. MODIS Collection 4 Active Fire Product User's Guide. Available on the Internet: 〈http://maps.geog.umd.edu/products/MODIS_Fire_Users_Guide_2.1.pdf〉.

Giglio, L., Descloitres, J., Justice, C.O., Kaufman, Y., 2003. An enhanced contextual fire detection algorithm for MODIS. Remote Sensing of Environment 87, 273–282.

Giglio, L., van der Werf, G.R., Randerson, J.T., Collatz, G.J., Kasibhatla, P.S., 2006. Global estimation of burned area using MODIS active fire observations. Atmospheric Chemistry and Physics 6, 957–974.

Hely, C., Caylor, K., Alleaume, S., Swap, R.J., Shugart, H.H., 2003. Release of gaseous and particulate carbonaceous compounds from biomass burning during the SAFARI 2000 dry season field campaign. Journal of Geophysical Research 108 (D13), 8470.

Hobbs, P.V., Reid, J.S., Kotchenruther, R.A., Ferek, R.J., Weiss, R., 1997. Direct radiative forcing by smoke from biomass burning. Science 275, 1776–1778.

Houghton, J.T., Ding, Y., Griggs, D.J., Noguer, M., van der Linden, P.J., Xiaosu, D. (Eds.), 2001. Climate Change 2001: The Scientific Basis. Cambridge University Press, Cambridge.

Ichoku, C., Kaufman, Y.J., 2005. A method to derive smoke emission rates from MODIS fire radiative energy measurements. IEEE Transactions on Geoscience and Remote Sensing 43 (11), 2636–2649.

Ito, A., Penner, J.E., 2004. Global estimates of biomass burning emissions based on satellite imagery for the year 2000. Journal of Geophysical Research 109, D14S05.

Justice, C.O., Vermote, E., Townshend, J.R.G., DeFries, R., Roy, D.P., Hall, D.P., Salomonson, V.V., Privette, J.L.,

Riggs, G., Strahler, A., Lucht, W., Myneni, R., Knyazikhin, Y., Running, S.W., Nemani, R.R., Wan, Z., Huete, A., van Leeuwen, W., Wolfe, R.E., Giglio, L., Muller, J.-P., Lewis, P., Barnsley, M.J., 1998. The moderate resolution imaging spectroradiometer (MODIS): land remote sensing for global change research. IEEE Transactions on Geoscience and Remote Sensing 36, 1228–1249.

Justice, C.O., Giglio, L., Korontzi, S., Owens, J., Morisette, J.T., Roy, D., Descloitres, J., Alleaume, S., Petitcolin, F., Kaufman, Y., 2002. The MODIS fire products. Remote Sensing of Environment 83, 244–262.

Kalnay, E., Kanamitsu, M., Kistler, R., Collins, W., Deaven, D., Gandin, L., Iredell, M., Saha, S., White, C., Woollen, J., Zhu, Y., Chelliah, M., Ebisuzaki, W., Higgins, W., Janowiak, J., Mo, K.C., Ropelewski, C., Wang, J., Leetmaa, A., Reynolds, R., Jenne, R., Joseph, D., 1996. The NCEP/NCAR 40-year reanalysis project. Bulletin of the American Meteorological Society 77 (3), 437–471.

Kaufman, Y.J., Fraser, R.S., 1997. The effect of smoke particles on clouds and climate forcing. Science 277, 1636–1639.

Kaufman, Y.J., Justice, C.O., 1998. Algorithm technical background document MODIS FIRE PRODUCTS, version 2.2, November 10 1998, EOS ID# 2741. NASA, Washington, D.C. 〈http://modis.gsfc.nasa.gov/data/atbd/atbd_mod14.pdf〉.

Kaufman, Y.J., Tanré, D., 1998. Algorithm for remote sensing of tropospheric aerosols from MODIS. MODIS Algorithm Theoretical Basis Document. Product ID: MOD04, Revised 26 October, 1998. Available on the Internet: 〈http://modis.gsfc.nasa.gov/data/atbd/atbd_mod02.pdf〉.

Kaufman, Y.J., Kleidman, R.G., King, M.D., 1998a. SCAR-B fires in the tropics: properties and remote sensing from EOS-MODIS. Journal of Geophysical Research 103, 31955–31968.

Kaufman, Y.J., Justice, C.O., Flynn, L., Kendall, J.D., Prins, E.M., Giglio, L., Ward, D.E., Menzel, W.P., Setzer, A.W., 1998b. Potential global fire monitoring from EOS-MODIS. Journal of Geophysical Research 103, 32215–32238.

Kaufman, Y.J., Tanré, D., Boucher, O., 2002. A satellite view of aerosols in the climate system. Nature 419, 215–223.

Kaufman, Y.J., Ichoku, C., Giglio, L., Korontzi, S., Chu, D.A., Hao, W.M., Li, R.-R., Justice, C.O., 2003. Fire and smoke observed from earth observing system MODIS instrument—products, validation, and operational use. International Journal of Remote Sensing 24, 1765–1781.

Keene, W.C., Lobert, J.M., Crutzen, P.J., Maben, J.R., Scharffe, D.H., Landmann, T., Hély, C., Brain, C., 2006. Emissions of major gaseous and particulate species during experimental burns of southern African biomass. Journal of Geophysical Research 111, D04301.

Kistler, R., Kalnay, E., Collins, W., Saha, S., White, G., Woollen, J., Chelliah, W., Ebisuzaki, W., Kanamitsu, M., Kousky, V., Dool, H., Jenne, R., Fiorino, M., 2001. The NCEP-NCAR 50-year reanalysis: monthly means CD-ROM and documentation. Bulletin of the American Meteorological Society 82, 247–267.

Korontzi, S., Roy, D.P., Justice, C.O., Ward, D.E., 2004. Modeling and sensitivity analysis of fire emissions in southern Africa during SAFARI 2000. Remote Sensing of Environment 92 (2), 255–275.

Levine, J.S., 1991. Global Biomass Burning: Atmospheric, Climatic, and Biospheric Implications. MIT Press, Cambridge, MA.

Levine, J.S., Cofer III, W.R., Cahoon Jr., D.R., Winstead, E.L., 1995. Biomass burning: a driver for global change. Environmental Science and Technology 29, 120–125.

Li, R.-R., Kaufman, Y.J., Hao, W.M., Salmon, J.M., Gao, B.C., 2004. A technique for detecting burn scars using MODIS data. IEEE Transactions on Geoscience and Remote Sensing 42 (6), 1300–1308.

Lighty, J.A., Veranth, J.M., Sarofim, A.F., 2000. Combustion aerosols: factors governing their size and composition and implications to human health. Journal of Air Waste Management Association 50, 1565–1618.

Logan, J.A., Prather, M.J., Wofsy, S.C., McElroy, M.B., 1981. Tropospheric chemistry: A global perspective. Journal of Geophysical Research 86, 7210–7254.

Malm, W.C., 1999. Introduction to Visibility (Air Resources Division, National Park Service, Cooperative Institute for Research in the Atmosphere [CIRA], NPS Visibility Program). Colorado State University, Fort Collins.

Malm, W.C., Hand, J.L., 2007. An examination of the physical and optical properties of aerosols collected in the IMPROVE program. Atmospheric Environment 41, 3407–3427.

Malm, W.C., Sisler, J.F., Huffman, D., Eldred, R.A., Cahill, T.A., 1994. Spatial and seasonal trends in particle concentration and optical extinction in the United States. Journal of Geophysical Research 99 (D1), 1347–1370.

Malm, W.C., Schichtel, B.A., Pitchford, M.L., Ashbaugh, L.L., Eldred, R.A., 2004. Spatial and monthly trends in speciated fine particle concentration in the United States. Journal of Geophysical Research 109, D03306.

NASA's Earth Observatory (EO), NASA News Archive, August 13, 2002. NASA's Terra Satellite Refines Map of Global Land Cover, Release No. 02-126. Available on the Internet: 〈http://www.earthobservatory.nasa.gov/Newsroom/LCC/〉.

Olson, J.S., 1981. Carbon balance in relation to fire regimes, USDA Forest Service Gen. Tech. Rep., WO-26, Washington, DC., 327–378.

Penman, J., Kruger, D., Galbally, I., Hiraishi, T., Nyenzi, B., Emmanul, S., Buendia, L., Hoppaus, R., Martinsen, T., Meijer, J., Miwa, K., Tanabe, K. (Eds.), 2000. Good Practice Guidance and Uncertainty Management in National Greenhouse Gas Inventories. IPCC, Institute for Global Environmental Strategies, Hayama, Japan. Available on the Internet: 〈http://www.ipcc-nggip.iges.or.jp/public/gp/english/〉.

Penner, J.E., Dickinson, R.E., O'Neill, C.A., 1992. Effects of aerosol from biomass burning on the global radiation budget. Science 256, 1432–1434.

Reid, S.B., Brown, S.G., Sullivan, D.C., Arkinson, H.L., Funk, T.H., Stiefer, P.S., 2004. Research and development of planned burning emission inventories for the Central States Regional Air Planning Association. Final Report Prepared for The Central States Air Resource Agencies and The Central Regional Air Planning Association, Oklahoma City, OK, by Sonoma Technology, Inc., Petaluma, CA, STI-902514-2516-FR. Available on the Internet: 〈http://www.dnr.missouri.gov/env/apcp/docs/d2-cenrap-plannedburn.pdf〉.

Reid, J.S., Koppmann, R., Eck, T.F., Eleuterio, D.P., 2005a. A review of biomass burning emissions, Part II: Intensive physical properties of biomass burning particles. Atmospheric Chemistry and Physics 5, 799–825.

Reid, J.S., Eck, T.F., Christopher, S.A., Koppmann, R., Dubovik, O., Eleuterio, D.P., Holben, B.N., Reid, E.A., Zhang, J., 2005b. A review of biomass burning emissions part

III: intensive optical properties of biomass burning particles. Atmospheric Chemistry and Physics 5, 827–849.

Roberts, G., Wooster, M.J., Perry, G.L.W., Drake, N., Rebelo, L-M., Dipotso, F., 2005. Retrieval of biomass combustion rates and totals from fire radiative power observations: Part 2—application to southern Africa using geostationary SEVIRI Imagery. Journal of Geophysical Research 110, D21111.

Robinson, J., 1989. On uncertainty in the computation of global emissions from biomass burning. Climatic Change 14.

Roy, D.P., Boschetti, L., O'Neal, K., 2006. MODIS Collection 5 Burned Area Product MCD45 User's Guide Version 1.0. Available on the Internet: 〈http://modis-fire.umd.edu/documents/MODIS_Burned_Area_Users_Guide_1.0.pdf〉.

Scholes, M., Andreae, M.O., 2000. Biogenic and pyrogenic emissions from Africa and their impact on the global atmosphere. Ambio 29 (1), 23–29.

Seiler, W., Crutzen, P.J., 1980. Estimates of gross and net fluxes of carbon between the biosphere and the atmosphere from biomass burning. Climatic Change 2, 207–247.

Simon, M., Plummer, S., Fierens, F., Hoelzemann, J.J., Arino, O., 2004. Burnt area detection at global scale using ATSR-2: the GLOBSCAR products and their qualification. Journal of Geophysical Research 109.

Soja, A.J., Cofer, W.R., Shugart, H.H., Sukhinin, A.I., Stackhouse Jr., P.W., McRae, D.J., Conard, S.G., 2004. Estimating fire emissions and disparities in boreal Siberia (1998–2002). Journal of Geophysical Research 109, D14S06.

van der Werf, G.R., Randerson, J.T., Giglio, L., Collatz, G.J., Kasibhatla, P.S., Arellano, A.F., 2006. Interannual variability in global biomass burning emissions from 1997 to 2004. Atmospheric Chemistry and Physics 6, 3423–3441.

Wang, J., Christopher, S.A., 2006. Mesoscale modeling of Central American smoke transport to the United States: 2. Smoke radiative impact on regional surface energy budget and boundary layer evolution. Journal of Geophysical Research 111, D14S92.

Wilson, C.L., Matthews, W.H. (Eds.), 1971. Report on the Study of Man's Impact on Climate (SMIC). Inadvertent Climate MIT Press, Cambridge.

Wolfe, R.E., Nishihama, M., Fleig, A.J., Kuyper, J.A., Roy, D.P., Storey, J.C., Patt, F.S., 2002. Achieving sub-pixel geolocation accuracy in support of MODIS land science. Remote Sensing of Environment 83, 31–49.

Wong, C.S., 1978. Atmospheric input of carbondioxide from burning wood. Science, 200. no. 4338, 197–200, doi:10.1126/science.200.4338.197.

Wooster, M.J., 2002. Small-scale experimental testing of fire radiative energy for quantifying mass combusted in natural vegetation fires. Geophysical Research Letters 29 (21), 2027.

Wooster, M.J., Zhukov, B., Oertel, D., 2003. Fire radiative energy for quantitative study of biomass burning: derivation from the BIRD experimental satellite and comparison to MODIS fire products. Remote Sensing of Environment 86, 83–107.

Wooster, M.J., Roberts, G., Perry, G.L.W., Kaufman, Y.J., 2005. Retrieval of biomass combustion rates and totals from fire radiative power observations: FRP derivation and calibration relationships between biomass consumption and fire radiative energy release. Journal of Geophysical Research 110, D24311.